Denver, Colorado
NOISE-CON 2013
2013 August 26-28

Experimental comparison of two active vibration control approaches: velocity feedback and negative capacitance shunt damping

Benjamin Beck
National Institute of Aerospace
100 Exploration Way
Hampton, VA 23666-6186
ben.beck@nasa.gov

Noah Schiller
MS 463
NASA Langley Research Center
Hampton, VA 23681

ABSTRACT

This paper outlines a direct, experimental comparison between two established active vibration control techniques. Active vibration control methods, many of which rely upon piezoelectric patches as actuators and/or sensors, have been widely studied, showing many advantages over passive techniques. However, few direct comparisons between different active vibration control methods have been made to determine the performance benefit of one method over another. For the comparison here, the first control method, velocity feedback, is implemented using four accelerometers that act as sensors along with an analog control circuit which drives a piezoelectric actuator. The second method, negative capacitance shunt damping, consists of a basic analog circuit which utilizes a single piezoelectric patch as both a sensor and actuator. Both of these control methods are implemented individually using the same piezoelectric actuator attached to a clamped Plexiglas window. To assess the performance of each control method, the spatially averaged velocity of the window is compared to an uncontrolled response.

1. INTRODUCTION

The use of thin, piezoelectric actuators to control vibrations on beams and panels has been of research interest for some time [1-3]. Active control approaches utilizing piezoelectric transducers have been shown to be an effective broadband solution to reducing vibration on panels [4], with many different architectures being researched. However, few direct comparisons have been made between active control approaches to determine the advantages and disadvantages. There has been research on piezoelectric vibration control compared to either constrained layer damping [5, 6], tuned mass dampers [7], and distributed vibration absorbers [6]. Similarly, many researchers have compared different implementations of switching shunt damping techniques [8-11]. This work focuses on a comparison of two separate active vibration control techniques in terms of suppression performance, power required for control, and the complexity of approach.

The two control methods that will be compared here are active damping and negative capacitance shunt control. Both of these methods utilize small, independent control units attached to a thin vibrating structure, and both approaches can be implemented using analog electronics. Active damping, or direct velocity feedback, uses matched sensor-actuator pairs to produce a control force that is directly proportional to velocity. For a sensor-actuator pair to be considered matched, they must couple to the system in the same way, e.g., a collocated point

sensor and a point force actuator. In practice, implementing a highly matched, collocated sensor-actuator pair is generally quite difficult. In this work, a piezoelectric actuator will be coupled with accelerometers as sensors. In contrast, negative capacitance shunt control uses a single piezoelectric transducer as both the sensor and actuator simultaneously. The negative capacitance shunt acts as a feedback controller that modifies the apparent impedance of the structure to reduce the global vibration amplitude. Therefore, the negative capacitance shunt control method is guaranteed to have a perfectly matched sensor-actuator pair due to the fact that it uses the same piezoelectric actuator as both the actuator and sensor. However even though both methods make use of different sensors, the performance of both active damping and negative capacitance shunt control will be compared using the same actuator. Another similarity between these two approaches is that both are implemented using analog electronics.

The rest of this work is organized into four sections. First, the control circuits are presented in detail along with the type of actuator that will be used for experimental comparison. Next, the experimental setup and procedures are outlined. The results, comparison, and analysis are then discussed. Finally, a conclusion of the comparison is made.

2. CONTROL CIRCUITS

Before outlining the control systems that will be compared, the actuator that will be utilized is first described. The type of actuator used is a diamond-shaped macro-fiber composite (MFC) piezoelectric transducer with integrated electrodes that has been previously developed by Schiller, Perey and Cabell [12]. Based on the triangular control actuators used in [13-15], the diamond-shaped MFC transducers improve performance over traditional piezoelectric triangular patches for use as control actuators by eliminating destabilizing edge and base line moments [12]. By using interdigitated electrodes instead of traditional, uniform bipolar electrodes, the edge line moments can be eliminated by choosing the slope of the diamond such that

$$m = \sqrt{\frac{-e_{12}}{e_{11}}} \tag{1}$$

where e_{ij} is the piezoelectric material constant relating the electric field in the i direction to the stress induced in the j direction. The base line moments can be negated by combining two triangular patches at their bases. By canceling the line moments, the diamond-shaped actuator couples to the system as four point forces at the four corners. Therefore, four point sensors must be utilized in the combination shown in Figure 1 to create a matched sensor for the diamond-shaped interdigitated piezoelectric transducer.

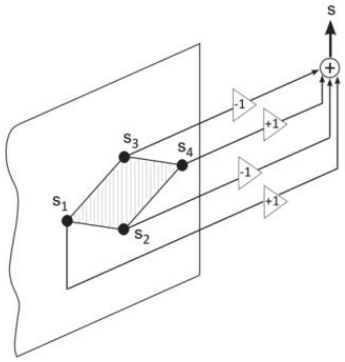

Figure 1 - Combination of point sensors to match the output response of the diamond shaped actuator

A. Active Damping Feedback System

The electrical components of the active damping feedback system include proper signal conditioning and amplification along with the control logic. Figure 2 shows a photograph of the complete active damping control circuit. Four IEPE (Integrated Electronics Piezo Electric) accelerometers are connected to the circuitry by four 10-32 connectors and are powered to the required 8 mA at 28 VDC. A high pass filter first removes this DC component from the accelerometer signals. The four individual sensor AC signals are scaled, summed, and integrated to obtain a signal value that is proportional to velocity. The overall gain of the controller is selected with an adjustable gain stage. The signal is then sent to two high voltage amplifiers to drive the piezoelectric actuator. For frequencies between 20 Hz and 20 kHz, the transfer function of input X to output voltage Y can be described as the simple model

$$\frac{Y(j\omega)}{X(j\omega)} = \frac{42,700\,jK}{f} \tag{2}$$

where f is the frequency and K is the adjustable gain with a range of 10 to 60. Outside of this frequency range, the actual transfer function deviates due to the high pass filters below 20 Hz and the limitations of the circuit components, specifically the op-amps, above 20 kHz. More details of the design and implementation of the circuit can be found in [12]. The gain K was set to 21.3 for this comparison, which was close to the highest value possible while retaining system stability.

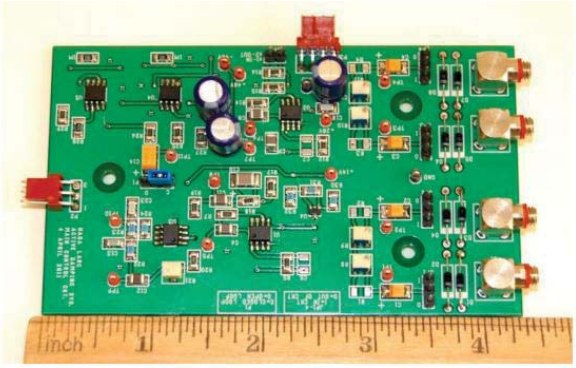

Figure 2 - Photograph of active damping control circuit [12].

B. Negative Capacitance Shunt

Shunts are any electrical device connected between the electrodes of a piezoelectric transducer used to modify the mechanical impedance of the system. Shunts are generally considered either passive or active based on their electrical components. One type of active shunt is the negative capacitance shunt. This type of shunt consists of a resistor and a negative capacitance element. The performance of the negative capacitance shunt can be described in terms of an active feedback controller [18]. For collocated drive and control transducers, the closed-loop transfer function between the voltage supplied to the system V_{in} and the voltage output of the control transducer V_p is

$$\frac{V_p}{V_{in}} = \frac{G(j\omega)}{1+G(j\omega)K(j\omega)} \tag{3}$$

where G is the open loop transfer function that encompasses the dynamics of the mechanical system. K is the controller transfer function including the impedance of the shunt, Z_S, and the impedance of the control transducer, Z_p, and is given by

$$K(j\omega) = \frac{Z_S(j\omega)}{Z_S(j\omega) + Z_p(j\omega)} \ . \tag{4}$$

Using a negative capacitance shunt with the impedance equal to Equation (6) and a control transducer with ideal capacitance, the controller becomes

$$K(j\omega) = \frac{j\omega - \frac{1}{R_S C_S}}{j\omega + \frac{1}{R_S C_S}\left(\frac{C_S}{C_P} - 1\right)} \tag{5}$$

where C_p is the capacitance of the control transducer, R_S is the shunt resistance, and C_S is the negative capacitance magnitude. It has been previously shown that the optimal value of shunt impedance to minimize vibration produces an undamped electrical response in the circuit, therefore $C_S > C_P$ to keep the electrical output of the op-amp within the supply voltage levels [18]. However, C_S should be as close to the value of C_P as possible to maximize control. The resistance value R_S determines the frequency bandwidth of control [19]. For this work, the value of negative capacitance was chosen to be 7.19 nF which is slightly larger than the transducer capacitance of 7.16 nF. The resistor was chosen to be 2000 Ω to allow for control in the frequency range of interest.

A negative impedance converter is used to create a negative capacitance element [16]. When combined with the series resistor, Figure 3a, the impedance of the shunt Z_S is defined as

$$Z_S = R_S + \frac{1}{-j\omega C_S} \tag{6}$$

where the negative capacitance can be found by

$$C_S = -\frac{R_4}{R_3} C_2 \ . \tag{7}$$

The resistors R_3 and R_4 are used to tune the negative capacitance value to the necessary magnitude. It should be noted that the large resistor R_2 is only added in parallel with the reference capacitor C_2 for low frequency op-amp stability but is not included in the definition of impedance because it is large enough to have negligible effect on the impedance above 10 Hz. Figure 3b shows a picture of a prototype negative capacitance circuit for comparison to the circuit used for implementation of active damping, Figure 2. The prototype circuit could be reduced in size with the use of surface mount electronics, however the size and number of components is significantly smaller than the active damping circuit.

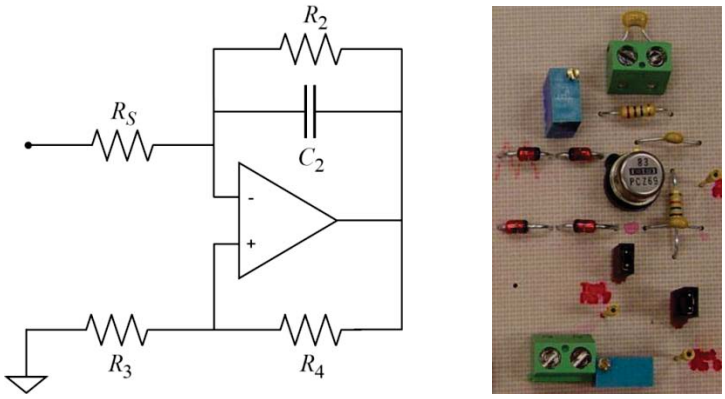

Figure 3 - Negative capacitance shunt a) schematic and b) photograph [17].

3. EXPERIMENTAL SETUP AND PROCEDURE

This section outlines the procedures and experimental setup that were used to compare the two control methods presented above. A Plexiglas window panel was utilized as the test structure. The physical properties of the window panel are shown in Table 1. A 12.8 cm long diamond-shaped transducer was placed in the center of the panel to act as the control actuator. The width of the actuator, 3.2 cm, was calculated from Equation (1). Refer to Schiller, Perey [12] for a photograph of the Plexiglas test panel. A smaller diamond-shaped actuator bonded on the opposite side of the panel from the control actuator, but in the same nominal position, was used to disturb the panel with a pseudorandom drive signal. Having the drive actuator substantially collocated with the control transducer ensured that only the modes that could be controlled would be excited, which allowed for a straightforward comparison of the two control approaches. Each circuit's op-amps were powered using two Sorensen DLM 20-30 power supplies which have built-in voltage and current meters allowing for the direct comparison of the total power delivered to the circuits. The two power supplies were connected in series to power each circuit and were necessary due to the fact that the op-amps require a DC voltage larger than the range of a single power supply.

Table 1 - Physical properties of Plexiglas window test panel

Thickness	4.45 mm
Height	90.4 cm
Width	70.9 cm
Mass	1.6 kg

The metric chosen to compare performance of the two active control circuits is the ability to suppress global vibration amplitude. This is quantified using the spatially averaged velocity-squared, $\left|v^2\right|$, which is proportional to the kinetic energy of the system. An 'open' case represents the uncontrolled response of the panel. The open response is compared to controlled responses with negative capacitance shunt alone and the active damping circuit alone. To simplify discussion of the results, the spatially averaged velocity-squared value at each frequency is normalized by the maximum squared velocity over all frequencies, or specifically the peak 'open' response is set to 0dB. A Polytec PSV-300 scanning laser Doppler vibrometer was used to determine the velocity at 420 points distributed over the surface of the Plexiglas window.

4. RESULTS AND ANALYSIS

Three criteria will be used to compare the two control approaches: suppression performance, power consumption, and approach complexity. The normalized spatially averaged velocity-squared for each control approach is compared to the uncontrolled open case to determine the suppression performance. Secondly, the power supplied to each control circuit during operation is compared. Finally, the complexity of each approach is described, which includes a discussion on cost and weight.

A. Suppression performance

Figure 4 shows the normalized spatially averaged velocity-squared magnitude versus frequency for the two control approaches and the open case. As can be seen, both active control approaches reduce the spatially averaged velocity of the panel; however the performance of the active damping circuit is significantly better. Specifically, the negative capacitance shunt reduces the magnitude at all resonance frequencies from 250 Hz to 2000 Hz and obtained a maximum reduction of 6.6 dB at 435 Hz. For the active damping approach, the bandwidth is greater: reductions are observed from 250 Hz to 3600 Hz. Similarly, the reduction in velocity is much larger than for the negative capacitance shunt for all frequencies in this bandwidth, with a maximum reduction of 21.5 dB at 435 Hz. However, due to spillover, there are two frequencies with increased response when the active damping control was applied: 2500 Hz and 5500 Hz with an increase in spatially averaged velocity-squared of 4.5 and 6.8 dB respectively.

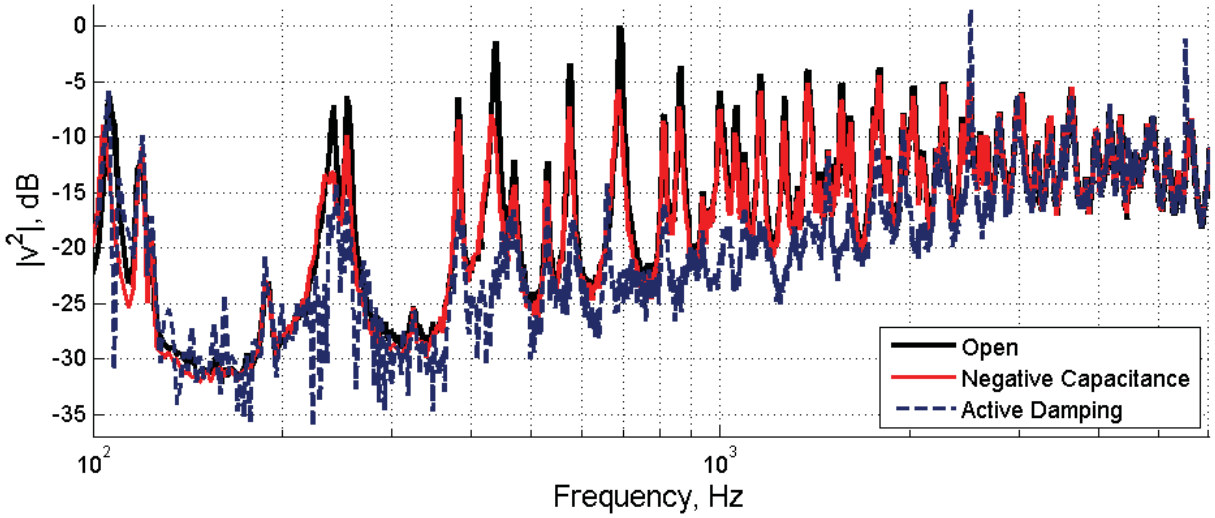

Figure 4 - Spatially averaged velocity-squared versus frequency

B. Power consumption

As stated in Section 3, the power supplied to the two circuits under operation was measured using the internal current and voltage meters inside the op-amp power supplies. The voltage, current and total power for each approach is shown in Table 2. The voltage shown is the differential voltage from the positive to the negative rail. Due to the low precision of the current meter, the current for the negative capacitance shunt was read to be 0.0 A. Therefore for the power computation, the current was assumed to be less than 0.05 A. It has been previously shown that the power necessary for the shunt is less than or equal to 1 W which validates this assumption [17]. Even assuming the highest possible power, the power consumed by the negative capacitance shunt is three times less than that of the active damping circuit.

Table 2 - Voltage, current, and power supplied to control approaches under use

Approach	Voltage (V)	Current (A)	Power (W)
Active Damping	28	0.25	7.0
Negative Capacitance Shunt	40	0.0*	< 2

C. Complexity

The complexity of each active control approach can be difficult to define and compare directly. There are significantly more electrical components used to create the active damping circuit, specifically the number of op-amps. In this circuit eight op-amps are used to combine and integrate the signals from the accelerometers and amplify the response. In contrast, only a single op-amp is used for the negative capacitance shunt. Another added complexity of the active damping system is that the sensors are separate from the actuators, which makes the performance of the system sensitive to the relative placement of each. However, the negative capacitance shunt utilizes the same transducer as the sensor and actuator, and therefore does not have the same placement sensitivity issues. Directly related to the number of components and sensing/actuation requirements is the cost of the components needed to implement each control approach. The number of electrical components increases the cost of the active damping circuit, but the significant cost of the four accelerometers for sensing makes the active damping approach at least one order of magnitude larger than the negative capacitance shunt approach. Therefore, it would be possible to increase the number of negative capacitance shunt units to improve control performance while still having fewer electrical components and less overall cost.

5. CONCLUSION

This paper has presented a direct experimental comparison of two active control approaches which suppress flexural vibrations. An active damping control approach and a negative capacitance shunt were first outlined. Each of these techniques was then implemented on a Plexiglas panel, and the performance of each was compared to the spatially averaged velocity of an uncontrolled case. It was shown that the active damping approach had significantly greater suppression performance than the negative damping shunt. Not surprisingly, the active damping circuit required at least three times the amount of power as the negative capacitance shunt. Lastly, the cost and complexity of the negative capacitance shunt is considerably less than that of the active damping approach. Therefore, based on these trade-offs of performance versus power and cost, the best active control approach is application specific.

6. REFERENCES

1. Bailey, T. and J.E. Hubbard, *Distributed Piezoelectric Polymer Active Vibration Control of a Cantilever Beam.* Journal of Guidance Control and Dynamics, 1985. **8**(5): p. 605-611.
2. Forward, R.L., *Electronic damping of vibrations in optical structures.* Applied Optics, 1979. **18**: p. 690-697.
3. Hagood, N.W. and A. von Flotow, *Damping of structural vibrations with piezoelectric materials and passive electrical networks.* Journal of Sound and Vibration, 1991. **146**(2): p. 243-68.
4. Fuller, C.C., S. Elliott, and P.A. Nelson, *Active control of vibration,* 1996: Academic Press.
5. Hollkamp, J.J. and R.W. Gordon, *An experimental comparison of piezoelectric and constrained layer damping.* Smart Materials & Structures, 1996. **5**(5): p. 715-722.

* Current was below meter precision, assumed to be 0.05 A.

6. Carneal, J.P., et al., *Re-Active Passive devices for control of noise transmission through a panel.* Journal of Sound and Vibration, 2008. **309**(3-5): p. 495-506.
7. Neubauer, M., R. Oleskiewicz, and K. Popp†, *Comparison of Damping Performance of Tuned Mass Dampers and Shunted Piezo Elements.* Pamm, 2005. **5**(1): p. 117-118.
8. Corr, L.R. and W.W. Clark, *Comparison of low-frequency piezoelectric switching shunt techniques for structural damping.* Smart Materials & Structures, 2002. **11**(3): p. 370-376.
9. Ducarne, J., O. Thomas, and J.F. Deu, *Structural Vibration Reduction by Switch Shunting of Piezoelectric Elements: Modeling and Optimization.* Journal of Intelligent Material Systems and Structures, 2010. **21**(8): p. 797-816.
10. Delpero, T., A.E. Bergamini, and P. Ermanni, *Identification of electromechanical parameters in piezoelectric shunt damping and loss factor prediction.* Journal of Intelligent Material Systems and Structures, 2012. **24**(3): p. 287-298.
11. Mokrani, B., et al., *Synchronized switch damping on inductor and negative capacitance.* Journal of Intelligent Material Systems and Structures, 2012. **23**(18): p. 2065-2075.
12. Schiller, N.H., D.F. Perey, and R.H. Cabell. *Development of a practical broadband active vibration control system*. in Proceedings of the *ASME International Mechanical Engineering Congress & Exposition*. 2011. Denver, CO, USA.
13. Gardonio, P. and S.J. Elliott, *Smart panels with velocity feedback control systems using triangularly shaped strain actuators.* The Journal of the Acoustical Society of America, 2005. **117**(4): p. 2046.
14. Aoki, Y., P. Gardonio, and S.J. Elliott, *Rectangular plate with velocity feedback loops using triangularly shaped piezoceramic actuators: experimental control performance.* J Acoust Soc Am, 2008. **123**(3): p. 1421-6.
15. Schiller, N.H., et al., *Active damping using distributed anisotropic actuators*, in *ASME International Mechanical Engineering Congress & Exposition*2010: Vancouver, BC, Canada.
16. Horowitz, P., W. Hill, and T.C. Hayes, *The art of electronics*. Vol. 2. 1989: Cambridge university press Cambridge.
17. Beck, B.S., *Negative Capacitance Shunting of Piezoelectric Patches for Vibration Control of Continuous Systems*, in *Mechanical Engineering*, 2012, Georgia Insitute of Technology: Georgia Institute of Technology.
18. Behrens, S., A.J. Fleming, and S.O.R. Moheimani, *A broadband controller for shunt piezoelectric damping of structural vibration.* Smart Materials & Structures, 2003. **12**(1): p. 18-28.
19. Beck, B., K.A. Cunefare, and M. Collet. *Broadband Vibration Suppression Assessment of Negative Impedance Shunts*. in Proceedings of the *ASME 2008 Conference on Smart Materials, Adaptive Structures and Intelligent Systems*. 2008. **1** Ellicott City, Maryland, USA.